

1.7. NONLINEAR OPTICAL PROPERTIES

with  $-\rho^+(\theta, \omega)$  for the positive class and  $+\rho^-(\theta, \omega)$  for the negative class.  $\rho^\pm(\theta, \omega)$  is given by

$$\rho^\pm(\theta, \omega) = \arccos(\mathbf{d}^\pm \cdot \mathbf{e}^\pm) = \arccos(\mathbf{u}^\pm \cdot \mathbf{s}^\pm) = \arccos \left\{ \left[ \frac{\cos^2 \theta}{n_o^2(\omega)} + \frac{\sin^2 \theta}{n_e^2(\omega)} \right] \left[ \frac{\cos^2 \theta}{n_o^4(\omega)} + \frac{\sin^2 \theta}{n_e^4(\omega)} \right]^{-1/2} \right\}. \tag{1.7.3.13}$$

Note that the extraordinary walk-off angle is nil for a propagation along the optic axis ( $\theta = 0$ ) and everywhere in the  $xy$  plane ( $\theta = \pi/2$ ).

1.7.3.1.4. Biaxial class

In a biaxial crystal, the three principal refractive indices are all different. The graphical representations of the index surfaces are given in Fig. 1.7.3.3 for the positive biaxial class ( $n_x < n_y < n_z$ ) and for the negative one ( $n_x > n_y > n_z$ ), both with the usual

conventional orientation of the optical frame. If this is not the case, the appropriate permutation of the principal refractive indices is required.

In the orthorhombic system, the three principal axes are fixed by the symmetry; one is fixed in the monoclinic system; and none are fixed in the triclinic system. The index surface of the biaxial class has two umbilici contained in the  $xz$  plane, making an angle  $V$  with the  $z$  axis:

$$\sin^2 V(\omega) = \frac{n_y^{-2}(\omega) - n_x^{-2}(\omega)}{n_z^{-2}(\omega) - n_x^{-2}(\omega)}. \tag{1.7.3.14}$$

The propagation along the optic axes leads to the internal conical refraction effect (Schell & Bloembergen, 1978; Fève *et al.*, 1994).

1.7.3.1.4.1. Propagation in the principal planes

It is possible to define ordinary and extraordinary waves, but only in the principal planes of the biaxial crystal: the ordinary electric field vector is perpendicular to the  $z$  axis and to the extraordinary one. The walk-off properties of the waves are not the same in the  $xy$  plane as in the  $xz$  and  $yz$  planes.

(1) In the  $xy$  plane, the extraordinary wave has no walk-off, in contrast to the ordinary wave. The components of the electric field vectors can be established easily with the same considerations as for the uniaxial class:

$$\begin{aligned} e_x^o &= -\sin[\varphi \pm \rho^\mp(\varphi, \omega)] \\ e_y^o &= \cos[\varphi \pm \rho^\mp(\varphi, \omega)] \\ e_z^o &= 0, \end{aligned} \tag{1.7.3.15}$$

with  $+\rho^-(\varphi, \omega)$  for the positive class and  $-\rho^+(\varphi, \omega)$  for the negative class.  $\rho^\pm(\varphi, \omega)$  is the walk-off angle given by (1.7.3.13), where  $\theta$  is replaced by  $\varphi$ ,  $n_o$  by  $n_y$  and  $n_e$  by  $n_x$ :

$$e_x^e = 0 \quad e_y^e = 0 \quad e_z^e = 1. \tag{1.7.3.16}$$

(2) The  $yz$  plane of a biaxial crystal has exactly the same characteristics as any plane containing the optic axis of a uniaxial crystal. The electric field vector components are given by (1.7.3.11) and (1.7.3.12) with  $\varphi = \pi/2$ . The ordinary walk-off is nil and the extraordinary one is given by (1.7.3.13) with  $n_o = n_y$  and  $n_e = n_z$ .

(3) In the  $xz$  plane, the optic axes create a discontinuity of the shape of the internal and external sheets of the index surface leading to a discontinuity of the optic sign and of the electric field vector. The birefringence,  $n_e - n_o$ , is nil along the optic axis, and its sign changes on either side. Then the  $yz$  plane,  $xy$  plane and  $xz$  plane from the  $x$  axis to the optic axis have the same optic sign, the opposite of the optic sign from the optic axis to the  $z$  axis. Thus a positive biaxial crystal is negative from the optic axis to the  $z$  axis. The situation is inverted for a negative biaxial crystal. It implies the following configuration of polarization:

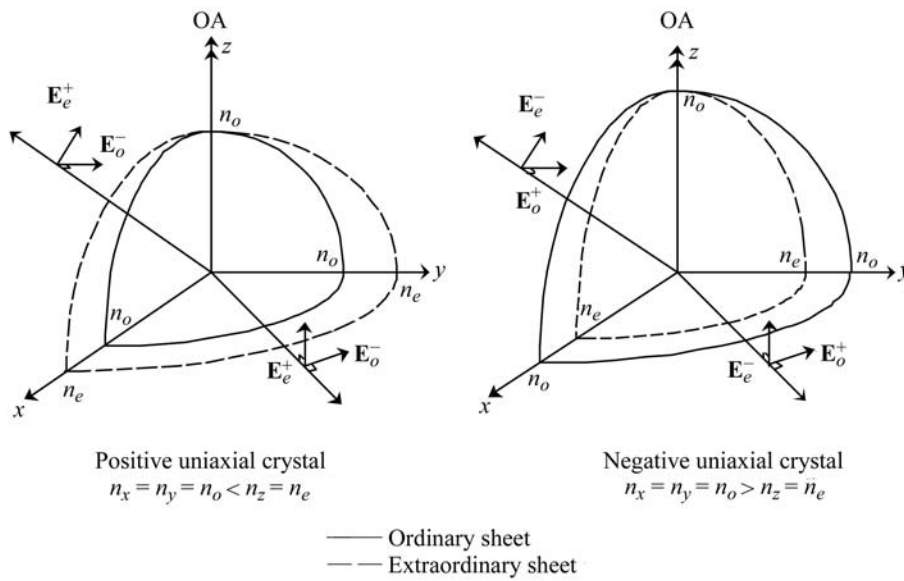


Fig. 1.7.3.2. Index surfaces of the negative and positive uniaxial classes.  $\mathbf{E}_{o,e}^\pm$  are the ordinary ( $o$ ) and extraordinary ( $e$ ) electric field vectors relative to the external (+) or internal (–) sheets. OA is the optic axis.

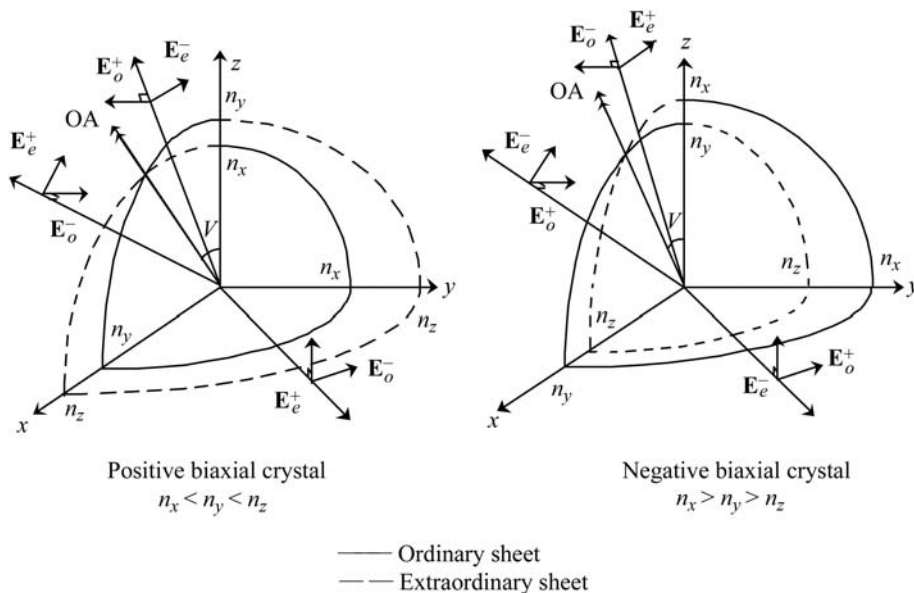


Fig. 1.7.3.3. Index surfaces of the negative and positive biaxial classes.  $\mathbf{E}_{o,e}^\pm$  are the ordinary ( $o$ ) and extraordinary ( $e$ ) electric field vectors relative to the external (+) or internal (–) sheets for a propagation in the principal planes. OA is the optic axis.

## 1. TENSORIAL ASPECTS OF PHYSICAL PROPERTIES

(i) From the  $x$  axis to the optic axis,  $\mathbf{e}^o$  and  $\mathbf{e}^e$  are given by (1.7.3.11) and (1.7.3.12) with  $\varphi = 0$ . The walk-off is relative to the extraordinary wave and is calculated from (1.7.3.13) with  $n_o = n_x$  and  $n_e = n_z$ .

(ii) From the optic axis to the  $z$  axis, the vibration plane of the ordinary and extraordinary waves corresponds respectively to a rotation of  $\pi/2$  of the vibration plane of the extraordinary and ordinary waves for a propagation in the areas of the principal planes of opposite sign; the extraordinary electric field vector is given by (1.7.3.12) with  $\varphi = 0$ ,  $-\rho^-(\varphi, \omega)$  for the positive class and  $+\rho^+(\varphi, \omega)$  for the negative class, and the ordinary electric field vector is out of phase by  $\pi$  in relation to (1.7.3.11), that is

$$e_x^o = 0 \quad e_y^o = -1 \quad e_z^o = 0. \quad (1.7.3.17)$$

The extraordinary walk-off angle is given by (1.7.3.13) with  $n_o = n_x$  and  $n_e = n_z$ .

The  $\pi/2$  rotation on either side of the optic axes is well observed during internal conical refraction (Fève *et al.*, 1994).

Note that for a biaxial crystal, the walk-off angles are all nil only for a propagation along the principal axes.

### 1.7.3.1.4.2. Propagation out of the principal planes

It is impossible to define ordinary and extraordinary waves out of the principal planes of a biaxial crystal: according to (1.7.3.6) and (1.7.3.9),  $\mathbf{e}^+$  and  $\mathbf{e}^-$  have a nonzero projection on the  $z$  axis. According to these relations, it appears that  $\mathbf{e}^+$  and  $\mathbf{e}^-$  are not perpendicular, so relation (1.7.3.10) is never verified. The walk-off angles  $\rho^+$  and  $\rho^-$  are nonzero, different, and can be calculated from the electric field vectors:

$$\rho^\pm(\theta, \varphi, \omega) = \varepsilon \arccos[\mathbf{e}^\pm(\theta, \varphi, \omega) \cdot \mathbf{u}(\theta, \varphi, \omega)] - \varepsilon\pi/2. \quad (1.7.3.18)$$

$\varepsilon = +1$  or  $-1$  for a positive or a negative optic sign, respectively.

### 1.7.3.2. Equations of propagation of three-wave and four-wave interactions

#### 1.7.3.2.1. Coupled electric fields amplitudes equations

The nonlinear crystals considered here are homogeneous, lossless, non-conducting, without optical activity, non-magnetic and are optically anisotropic. The nonlinear regime allows interactions between  $\gamma$  waves with different circular frequencies  $\omega_i, i = 1, \dots, \gamma$ . The Fourier component of the polarization vector at  $\omega_i$  is  $\mathbf{P}(\omega_i) = \varepsilon_0 \chi^{(1)}(\omega_i) \mathbf{E}(\omega_i) + \mathbf{P}^{NL}(\omega_i)$ , where  $\mathbf{P}^{NL}(\omega_i)$  is the nonlinear polarization corresponding to the orders of the power series greater than 1 defined in Section 1.7.2.

Thus the propagation equation of each interacting wave  $\omega_i$  is (Bloembergen, 1965)

$$\nabla_x \nabla_x \mathbf{E}(\omega_i) = (\omega_i^2/c^2) \varepsilon(\omega_i) \mathbf{E}(\omega_i) + \omega_i^2 \mu_0 \mathbf{P}^{NL}(\omega_i). \quad (1.7.3.19)$$

The  $\gamma$  propagation equations are coupled by  $\mathbf{P}^{NL}(\omega_i)$ :

(1) for a three-wave interaction,  $\gamma = 3$ ,

$$\mathbf{P}^{NL}(\omega_1) = \mathbf{P}^{(2)}(\omega_1) = \varepsilon_0 \chi^{(2)}(\omega_1 = \omega_3 - \omega_2) \cdot \mathbf{E}(\omega_3) \otimes \mathbf{E}^*(\omega_2),$$

$$\mathbf{P}^{NL}(\omega_2) = \mathbf{P}^{(2)}(\omega_2) = \varepsilon_0 \chi^{(2)}(\omega_2 = \omega_3 - \omega_1) \cdot \mathbf{E}(\omega_3) \otimes \mathbf{E}^*(\omega_1),$$

$$\mathbf{P}^{NL}(\omega_3) = \mathbf{P}^{(2)}(\omega_3) = \varepsilon_0 \chi^{(2)}(\omega_3 = \omega_1 + \omega_2) \cdot \mathbf{E}(\omega_1) \otimes \mathbf{E}^*(\omega_2);$$

(2) for a four-wave interaction

$$\mathbf{P}^{NL}(\omega_1) = \mathbf{P}^{(3)}(\omega_1) = \varepsilon_0 \chi^{(3)}(\omega_1 = \omega_4 - \omega_2 - \omega_3) \cdot \mathbf{E}(\omega_4) \otimes \mathbf{E}^*(\omega_2) \otimes \mathbf{E}^*(\omega_3),$$

$$\mathbf{P}^{NL}(\omega_2) = \mathbf{P}^{(3)}(\omega_2) = \varepsilon_0 \chi^{(3)}(\omega_2 = \omega_4 - \omega_1 - \omega_3) \cdot \mathbf{E}(\omega_4) \otimes \mathbf{E}^*(\omega_1) \otimes \mathbf{E}^*(\omega_3),$$

$$\mathbf{P}^{NL}(\omega_3) = \mathbf{P}^{(3)}(\omega_3) = \varepsilon_0 \chi^{(3)}(\omega_3 = \omega_4 - \omega_1 - \omega_2) \cdot \mathbf{E}(\omega_4) \otimes \mathbf{E}^*(\omega_1) \otimes \mathbf{E}^*(\omega_2)$$

$$\mathbf{P}^{NL}(\omega_4) = \mathbf{P}^{(3)}(\omega_4) = \varepsilon_0 \chi^{(3)}(\omega_4 = \omega_1 + \omega_2 + \omega_3) \cdot \mathbf{E}(\omega_1) \otimes \mathbf{E}(\omega_2) \otimes \mathbf{E}(\omega_3).$$

The complex conjugates  $\mathbf{E}^*(\omega_i)$  come from the relation  $\mathbf{E}^*(\omega_i) = \mathbf{E}(-\omega_i)$ .

We consider the plane wave, (1.7.3.3), as a solution of (1.7.3.19), and we assume that all the interacting waves propagate in the same direction  $Z$ . Each linearly polarized plane wave corresponds to an eigen mode  $\mathbf{E}^+$  or  $\mathbf{E}^-$  defined above. For the usual case of beams with a finite transversal profile and when  $Z$  is along a direction where the double-refraction angles can be nonzero, *i.e.* out of the principal axes of the index surface, it is necessary to specify a frame for each interacting wave in order to calculate the corresponding powers as a function of  $Z$ : the coordinates linked to the wave at  $\omega_i$  are written  $(X_i, Y_i, Z)$ , which can be relative to the mode (+) or (-). The systems are then linked by the double-refraction angles  $\rho$ : according to Fig. 1.7.3.1, we have  $X_j^+ = X_i^+ + Z \tan[\rho^+(\omega_j) - \rho^+(\omega_i)]$ ,  $Y_j^+ = Y_i^+$  for two waves (+) with  $\rho^+(\omega_j) > \rho^+(\omega_i)$ , and  $X_j^- = X_i^-$ ,  $Y_j^- = Y_i^- + Z \tan[\rho^-(\omega_j) - \rho^-(\omega_i)]$  for two waves (-) with  $\rho^-(\omega_j) > \rho^-(\omega_i)$ .

The presence of  $\mathbf{P}^{NL}(\omega_i)$  in equations (1.7.3.19) leads to a variation of the  $\gamma$  amplitudes  $E(\omega_i)$  with  $Z$ . In order to establish the equations of evolution of the wave amplitudes, we assume that their variations are small over one wavelength  $\lambda_i$ , which is usually true. Thus we can state

$$\begin{aligned} \frac{1}{k(\omega_i)} \left| \frac{\partial E(\omega_i, X_i, Y_i, Z)}{\partial Z} \right| &\ll |E(\omega_i, X_i, Y_i, Z)| \text{ or} \\ \left| \frac{\partial^2 E(\omega_i, X_i, Y_i, Z)}{\partial Z^2} \right| &\ll k(\omega_i) \left| \frac{\partial E(\omega_i, X_i, Y_i, Z)}{\partial Z} \right|. \end{aligned} \quad (1.7.3.20)$$

This is called the slowly varying envelope approximation.

Stating (1.7.3.20), the wave equation (1.7.3.19) for a forward propagation of a plane wave leads to

$$\begin{aligned} \frac{\partial E(\omega_i, X_i, Y_i, Z)}{\partial Z} &= j\mu_0 \frac{\omega_i^2}{2k(\omega_i) \cos^2 \rho(\omega_i)} \mathbf{e}(\omega_i) \cdot \mathbf{P}^{NL}(\omega_i, X_i, Y_i, Z) \\ &\times \exp[-jk(\omega_i)Z]. \end{aligned} \quad (1.7.3.21)$$

We choose the optical frame  $(x, y, z)$  for the calculation of all the scalar products  $\mathbf{e}(\omega_i) \cdot \mathbf{P}^{NL}(\omega_i)$ , the electric susceptibility tensors being known in this frame.

For a three-wave interaction, (1.7.3.21) leads to

$$\begin{aligned} \frac{\partial E_1(X_1, Y_1, Z)}{\partial Z} &= j\kappa_1 [\mathbf{e}_1 \cdot \varepsilon_0 \chi^{(2)}(\omega_1 = \omega_3 - \omega_2) \cdot \mathbf{e}_3 \otimes \mathbf{e}_2] \\ &\times E_3(X_3, Y_3, Z) E_2^*(X_2, Y_2, Z) \exp(j\Delta k Z) \\ \frac{\partial E_2(X_2, Y_2, Z)}{\partial Z} &= j\kappa_2 [\mathbf{e}_2 \cdot \varepsilon_0 \chi^{(2)}(\omega_2 = \omega_3 - \omega_1) \cdot \mathbf{e}_3 \otimes \mathbf{e}_1] \\ &\times E_3(X_3, Y_3, Z) E_1^*(X_1, Y_1, Z) \exp(j\Delta k Z) \\ \frac{\partial E_3(X_3, Y_3, Z)}{\partial Z} &= j\kappa_3 [\mathbf{e}_3 \cdot \varepsilon_0 \chi^{(2)}(\omega_3 = \omega_1 + \omega_2) \cdot \mathbf{e}_1 \otimes \mathbf{e}_2] \\ &\times E_1(X_1, Y_1, Z) E_2(X_2, Y_2, Z) \exp(-j\Delta k Z), \end{aligned} \quad (1.7.3.22)$$

with  $\mathbf{e}_i = \mathbf{e}(\omega_i)$ ,  $E_i(X_i, Y_i, Z) = E(\omega_i, X_i, Y_i, Z)$ ,  $\kappa_i = (\mu_0 \omega_i^2) / [2k(\omega_i) \cos^2 \rho(\omega_i)]$  and  $\Delta k = k(\omega_3) - [k(\omega_1) + k(\omega_2)]$ , called the phase mismatch. We take by convention  $\omega_1 < \omega_2 (< \omega_3)$ .